



## A Barrier Function-Based Integral Sliding Mode Control of Heart Rate During Treadmill Exercise

Taghreed MohammadRidha<sup>\*</sup>, Shibly Ahmed Al-Samarraie<sup>†</sup>

Control and Systems Engineering Department, University of Technology – Iraq, Baghdad 10066, Iraq

Corresponding Author Email: [taghreed.m.ridha@uotechnology.edu.iq](mailto:taghreed.m.ridha@uotechnology.edu.iq)

<https://doi.org/10.18280/mmep.100120>

### ABSTRACT

**Received:** 31 July 2022

**Accepted:** 20 January 2023

#### Keywords:

*heart rate control, cardiovascular system, exercise, integral sliding mode control, barrier function, nonlinear systems, reference tracking*

The objective of this work is to design an Integral Sliding Mode Controller based on barrier function (ISMcbf) for a human Heart Rate (HR) during a treadmill exercise. ISMcbf commands the speed of the treadmill such that the individual HR follows a time-varying profile. This profile is pre specified as part of rehabilitation exercises for patients with cardiovascular diseases. ISMcbf is chosen due to its well-known robustness properties as well as to its simple design procedure as compared to classic SMC and ISMC. It does not require the upper bounds of the uncertainties and perturbations in its design. Moreover, it does not have discontinuous function, hence it is a chattering-free controller. ISMcbf designed in this work for the first time for this system and its performance is compared to Quasi SMC (QSMC) and Super Twisting SMC (STSMC) from previous studies. The simulated exercises were conducted on a nonlinear model describing HR response to the walking speed of a treadmill. For ISMcbf, the model parameters and their upper bound of uncertainties are considered unknown. During two different exercise scenarios, the three controllers guided HR to follow the time-varying reference profile. However, ISMcbf showed higher quantitative performance by recording less Integral Squared Error (ISE) and Integral Time Absolute Error (ITAE) indices as compared to the other controllers.

## 1. INTRODUCTION

Cardiovascular diseases (CVDs) are the first main cause of death representing 32% of all global deaths in 2019 according to the World Health Organization (WHO) [1]. The study underlined that cardiovascular events could be prevented by addressing behavioral risk factors like physical inactivity. Many studies showed that Cardiac Rehabilitation (CR) represents an important secondary prevention model that can contribute favourably to the reduction of mortality and disability [2]. A CR program includes many elements like educational sessions on different topics such as risk factors. An important element of CR programs is the physical exercise that help improving physical capacity and fitness. During dynamic exercise, the metabolic demand increases, which in turn increases the Heart Rate (HR) and stroke volume. Different mathematical models were developed in the literature [3-5] to predict HR response during exercises. Modelling HR kinetics helps understanding the system behavior and provides some useful means for the prevention of cardiac failure [3]. Ludwig et al. [6] presented an overview of measurement, prediction, and control of individual HR responses. Available sensor technologies measuring HR are analyzed and the feasibility for wearables is analyzed as well. Wang and Hunt [7] investigated the linear second-order models of HR response to the available linear first-order models. They performed experimental tests on eleven participants each performed two open-loop identification tests while running at moderate-to-vigorous intensity on a treadmill. The authors concluded that second-order models

give significantly better fitting performance than first-order models. A similar comparison of first and second-order models of HR of cycle-ergometer was performed in the study of Spörri et al. [8]. However, physiological systems like HR response to exercise are known to exhibit nonlinear behaviors. One of the nonlinear models that can capture HR dynamic behavior using a reduced number of parameters is the one of [3] that is frequently used in the literature for control design. This model that describes HR response to the speed of a treadmill is also applicable to represent HR response to the speed of cycle-ergometer [9]. Moreover, it was also shown in the study of Liu et al. [10] that it can also well describe HR response in the outdoor running exercise by re-identifying its parameters.

The main purpose of HR models is to precisely control HR response to follow a pre-specified profile prescribed for healthy subjects like athletes or for patients of cardiovascular problems. A nonlinear controller was designed in the study of Scalzi et al. [11] for the nonlinear HR model given in the study of Cheng et al. [3] during a treadmill exercise. The authors considered it as a generalization of the classical proportional-integral controller that was designed in the literature for linear HR models. This nonlinear controller is also used in the study of Paradiso et al. [9] to control HR during cycle-ergometer exercises at constant cycling speed. Adaptive  $H_\infty$  controller is designed in the study of Baig et al. [12] to control HR response during aerobic activities of unknown type. The  $H_\infty$  controller is designed based on Linear Time-Varying (LTV) model. The controller is adaptively re-designed after three sampling intervals based on the estimation of the LTV model parameters

at every sampling time.

Sliding Mode Control (SMC) has its share here for HR control due to its well-known robustness. An event-driven Adaptive Integral Sliding Mode Control (AISMC) is designed in the study of Argha et al. [13] to control the HR during a cycle-ergometer exercise. Their results were based on a LTV first order HR model. They used a model-based disturbance estimator that is employed in the control law. Quasi SMC (QSMC) is designed in the study of Sarkar and Sengupta [14] and tested on the nonlinear model of Cheng et al. [3] where they approximated the discontinuous term of SMC by a continuous sigmoid function to avoid chattering. The control law used the nominal system parameters in the control law and was simulated on one case study only. It was shown that SMC performed better than an existing controller from the literature. In other study, Esmaili et al. [15] designed a Super-Twisting based SMC (STSMC) to track a pre-defined HR profile. They employed particle swarm optimization to re-identify the nonlinear model of the research [3] on ten subjects. The parameter estimation was realized for a larger treadmill speeds in the range (2-14 km/h).

Most of the previous studies either estimated the model parameters/disturbances or used the knowledge of its upper bounds in the design. Recently, a new barrier function based SMC design strategy is proposed by Obeid et al. [16] for a class of disturbed systems. Unlike SMC designs in previous studies, the proposed control approach does not require prior knowledge of the parameters uncertainty and/or perturbations bounds.

In this work, ISMC based on barrier function (ISMcbf) is designed for the first time to control HR during treadmill exercise. Barrier function based SMC and ISMC was successfully applied in several applications and proved its efficiency [17-19]. The main contributions of this work are:

1. ISMCbf is designed and tested on the nonlinear HR model during large range of treadmill speeds for the first time.
2. Prior knowledge of the model parameters uncertainty bounds are not required in the design. Once ISMCbf is designed, it is applied on different unknown sets of model parameters (different subjects).
3. Employing ISMC has the advantage over classical SMC that the sliding motion occurs from the first instant. Adding the barrier function with ISMC identifies the invariant neighborhood of the sliding manifold using one small positive parameter. Hence, the state trajectory is immediately confined in the invariant barrier neighborhood around the sliding surface.
4. The steady-state error and output accuracy is predefined by the barrier function small positive parameter. The barrier neighborhood is an invariant set to confine the state trajectory inside it. Hence, the barrier function based design has stronger robustness properties.
5. ISMCbf is continuous and chattering-free since the barrier function is differentiable.

To show the efficiency of the proposed approach, ISMCbf is compared to other controllers designed in previous studies: QSMC [14] and STSMC [15]. This comparison is useful as QSMC outperformed an existing reference controller and STSMC outperformed PID performance that was designed in another earlier study. Both studies were tested on the nonlinear model of Cheng et al. [3]. In this work, ISMCbf, QSMC and STSMC are tested on the nonlinear model to control HR response during treadmill exercise to track a predefined time-varying reference trajectory.

This paper is organized as follows: Next section is dedicated to the system model description. Section 3 presents the controller design and stability analysis. Section 4 illustrates the simulation results and comparison with controllers from the literature. Conclusions are presented in Section 5.

## 2. MODEL DESCRIPTION AND PROBLEM FORMULATION

The following nonlinear model describes HR response to the treadmill speed during an exercise [15, 11, 3]:

$$\left. \begin{aligned} \dot{x}_1 &= -a_1x_1 + a_2x_2 + a_3v^2 \\ \dot{x}_2 &= -a_4x_2 + \phi(x_1) \\ y &= 4x_1 + HR_o \end{aligned} \right\} \quad (1)$$

where,  $\phi(x_1) = \frac{a_5x_1}{1+e^{-(x_1-a_6)}}$ ,  $x_1$  is proportional to the deviation of HR from its value at rest ( $HR_o$ ),  $y$  is related to the at-rest and measured HR in beats per minute (bpm) [3, 11],  $u$  is the treadmill speed control input in km/h, and  $a_i, i=1, \dots, 6$  are positive parameters to represent a particular HR response per individual. The time  $t$  is measured in minutes. According to this model, HR is proportional to the square of the treadmill running speed. HR response is also affected by slower effects like body temperature and peripheral metabolism. These effects that arises during the running exercise and act as a disturbance on  $x_1$  and are represented in the model by  $x_2$ . The latter dynamics have an increasing effect on  $x_1$  during exercise since  $x_2 \geq 0$  and  $a_2 > 0$ .

## 3. CONTROL DESIGN

In this section, a robust controller was proposed based on the theory of integral sliding mode control. The concept of ISMC is presented in the first part of this section. In the second part, the proposed control design is introduced using the system dynamic model which is given in Eq. (1). Lastly, the proposed control system was proved using the input-to-state stability property.

### 3.1 Integral sliding mode control based on barrier function

In conventional sliding mode control, the robustness property with respect to the variations of system parameters and external disturbances can only be achieved during the sliding mode [20]. However, during the reaching phase, there is no guarantee for robustness. Eliminating the reaching phase in SMC can be achieved via the integral sliding mode, where the state is in the sliding phase from the first instant [20]. The ISMC approach was proposed so in researches [21, 22]. It is also named the Full Order Sliding Mode Control, because the system order during sliding mode does not change, unlike the conventional SMC, the system order is reduced by the control inputs number. However, the control system dynamic model is certain during the sliding motion for the traditional SMC and ISMC.

To illustrate the concept of the ISMC, let us consider the following scalar control system:

$$\dot{x} = f(x) + g(x) + h(t, x), \quad g(x) > 0 \quad \forall x \quad (2)$$

where,  $x \in R, f \in R, g \in R, u \in R$  and  $h \in R$  is the perturbation which represents the uncertainty in system model and the external disturbances.

Note that when  $h(x,t)=0$ , the system model in Eq. (2) becomes certain or nominal system model.

Assume that  $h(x,t)$  satisfies the matching condition  $h(x,t) = g(x)\hat{h}(x,t)$ . Then Eq. (2) is given by:

$$\dot{x} = f(x) + g(x)(u + \hat{h}(x,t)) \quad (3)$$

Let us take the control  $u$  as:

$$u = u_n + u_s \quad (4)$$

where,  $u_n$  is the nominal control, while  $u_s$  is the discontinuous control. Also let the sliding variable  $s$  be defined as;

$$s = x + z \quad (5)$$

where,  $z \in R$  is an additional state which added in order to eliminate the reaching phase with certain initial condition. So by selecting  $z(0)=-x(0)$ , the sliding phase starts from  $t \geq 0$ . Moreover, and as mentioned above, the system is certain for all  $t \geq 0$ . This can be proved below via equivalent control approach [23], where the closed loop system is assumed in ideal sliding mode.

Firstly, the sliding variable dynamics is obtained as:

$$\begin{aligned} \dot{s} &= \dot{x} + \dot{z} = f(x) + g(x)(u + \hat{h}(x,t)) + \dot{z} \\ &= f(x) + g(x)u_n + g(x)(u_s + \hat{h}(x,t)) + \dot{z} \end{aligned} \quad (6)$$

Then the dynamics of  $z$  is selected as the research [20]:

$$\dot{z} = -f(x) - g(x)u_n \quad (7)$$

Hence,

$$\dot{s} = g(x)(u_s + \hat{h}(x,t)) \quad (8)$$

In the equivalent mode,  $\dot{s} = 0$ , which leads to:

$$[\dot{s}]_{equivalent} = g(x)([u_s]_{equivalent} + \hat{h}(x,t)) = 0 \quad (9)$$

That means the discontinuous control  $u_s$ , in the equivalent mode ( $[u_s]_{equivalent}$ ), will eliminate the perturbation term. This will occur from the first instant ( $t \geq 0$ ). Note that the equivalent mode is the system response which is equivalent to the system response under the discontinuous control [23]. Consequently, from Eq. (2), the equivalent closed loop-control system is given by:

$$\dot{x} = f(x) + g(x)u_n, \forall t \geq 0 \quad (10)$$

So as can be seen from Eq. (10), the control system model is the nominal system model and the control  $u_n$  can be designed to give the desired system characteristics from the first instant.

For the discontinuous control  $u_s$ , its form in the conventional SMC (CSMC) is given by:

$$u_s|_{CSMC} = -k * \text{sign}(s) \quad (11)$$

The Barrier Function is then used in  $u_s$  instead of the discontinuous form given in Eq. (11). For the ISMC law based on using barrier function (ISMcbf),  $u_s$  can take the following form:

$$u_s|_{ISMcbf} = -\lambda_s \frac{s}{\epsilon - |s|} \quad (12)$$

where  $\epsilon > 0$  represents the thickness of the boundary layer, while  $\lambda_s > 0$  is the control gain which will be selected to enhance the control robustness and adjust the steady state error. To this end, in the ISMC, the use of  $u_s|_{ISMcbf}$  instead of  $u_s|_{CSMC}$  has great features which can be summarized as follows;

- For  $u_s|_{CSMC}$  we need to determine the value of  $k$  which requires knowing the bound on the uncertainty of system model. While for  $u_s|_{ISMcbf}$  any information about the model uncertainty is no longer needed.
- Since  $u_s|_{ISMcbf}$  is a continuous control law inside the boundary layer ( $|s| < \epsilon$ ), the chattering in the control system response is attenuated (or eliminated), while for the case of  $u_s|_{ISMcbf}$  and due to the conservative determination of the gain  $k$ , the chattering exists and maybe with high amplitude.

Note that the chattering is the main problem in the SMC system which appears in the control system response due to the use of a discontinuous control law as in  $u_s|_{CSMC}$  [24].

### 3.2 ISMCbf design using input-output model

The robust controller design for HR during treadmill exercise system is presented here. The proposed controller was based on the input-output model, where the output, which was used here, is the error function. It is defined as the difference between the reference and the actual values of the output  $y$  in Eq. (1). The error function is given by;

$$e = y_r - y \quad (13)$$

where,  $y_r$  is the reference (or desired) value of  $y$ , while the input is  $u = v^2$  (see Eq. (1)). So, according to the nonlinear model described in Eq. (1), the input-output model is obtained as;

$$\dot{e} = \dot{y}_r - \dot{y} = \dot{y}_r + \hat{a}_1 x_1 - \hat{a}_2 x_2 - \hat{a}_3 u \quad (14)$$

where,  $\hat{a}_i = 4a_i > 0, i = \{1,2,3\}$ .

**Remark 1:** For this input-output model, since the control input is a positive quantity, then  $u$  must be taken zero when the error function  $e \leq 0$ .

This remark can be proved via the following Lyapunov function;

$$V(e) = \frac{1}{2} e^2 \quad (15)$$

The time derivative of  $V(e)$  is:

$$\dot{V}(e) = e\dot{e} = e(\dot{y}_r + \hat{a}_1 x_1 - \hat{a}_2 x_2) - \hat{a}_3 eu \quad (16)$$

Therefore, when  $e > 0$ ,  $\hat{a}_3 eu$  will be a positive value and the

control system will make the origin of the error space an attractive point. On the other hand, when  $e \leq 0$ , the control input  $u$  must be taken zero, otherwise,  $\hat{a}_3 e u$  will be a negative value, and then it will not help the origin to be an attractive point.

According to the above, two regions are obtained; the first is  $\mathcal{Q}^{(+)}$  when  $e > 0$ , which is the closed loop region ( $u \neq 0$ ); and the second is  $\mathcal{Q}^{(-)}$  when  $e \leq 0$  the open loop region ( $u = 0$ ).

In this work, the proposed controller utilizes the ISMC based on the barrier function (ISMcbf). Therefore, as in Eqns. (4) and (5), the controller  $u$  and the sliding variable  $s$  are given as follows:

$$u = u_n + u_s \quad (17)$$

where,  $u_n$  is the nominal control, while  $u_s$  is the discontinuous control term. And:

$$s = e + z \quad (18)$$

where,  $z$  is an auxiliary variable, with the initial condition  $z(0) = -e(0)$  i.e.  $s(0) = 0$ , which means that the reaching phase is eliminated, because initially the state is at the sliding manifold  $s = 0$ . The controller design in the next steps is for the case where  $e > 0$  (the error state initiated in  $\mathcal{Q}^{(+)}$ ); otherwise  $u = 0$  if  $e \leq 0$ . Firstly, we need to derive the control law for  $u_n$  for the case where  $e > 0$  (the error state initiated in  $\mathcal{Q}^{(+)}$ ), we need to determine the dynamic of the sliding variable. To do that, from Eq. (14),  $\dot{e}$  is rewritten as the sum of a certain and an uncertain term,

$$\dot{e} = -Gu + H(x, u) = -Gu_n - Gu_s + H(x, u) \quad (19)$$

where,  $G = \hat{a}_{3n} = 4a_{3n} > 0$  is the control gain, and  $\hat{a}_{3n}$  is the nominal value of  $\hat{a}_3$ , while  $H(x, u)$  represents the uncertainty in Eq.(19) which includes the uncertainty in  $a_3 u (\delta \hat{a}_3 u)$ , i.e.,

$$H(x, u) = \dot{y}_r + \hat{a}_1 x_1 - \hat{a}_2 x_2 - \delta \hat{a}_3 u \quad (20)$$

Therefore, from Eqns. (17) to (19),  $\dot{s}$  is obtained as;

$$\dot{s} = \dot{e} + \dot{z} = -Gu_n + \dot{z} - Gu_s + H(x, u) \quad (21)$$

Based on the theory of ISMC, which was introduced [20], the dynamics of  $z$  is given by:

$$\dot{z} = Gu_n \quad (22)$$

So,  $\dot{s}$  becomes;

$$\dot{s} = -Gu_s + H(x, u) \quad (23)$$

Based on using the equivalent control theory,

$$[u_s]_{\text{equivalent}} = \frac{H(x, u)}{G} \quad (24)$$

As a result, from the first instant the error dynamics in Eq. (19) equivalently becomes;

$$\dot{e} = -Gu_n, \quad t \geq 0 \quad (25)$$

Therefore, the nominal control  $u_n$  is designed such that the

error dynamics takes the desired exponential decay rate. That means:

$$u_n = \lambda_n e / G \quad (26)$$

where,  $\lambda_n > 0$ . In addition, from Eq. (12),  $u_s$  can be taken as:

$$u_s = \frac{\lambda_s s}{G \epsilon - |s|} \quad (27)$$

Before presenting the proposed controller, we need to define the positive function  $[w]_+$  as follows.

**Definition 1:** The positive function  $[w]_+$ , is defined by;

$$[w]_+ = \begin{cases} 1 & \text{if } w > 0 \\ 0 & \text{if } w \leq 0 \end{cases}$$

The need for using the positive function is clarified in the following proposition.

**Proposition 1:** For the HR response during treadmill exercise model (Eq. (1)), the control law:

$$u = u_n + u_s = \frac{1}{G} \left\{ \lambda_n e + \lambda_s \frac{s}{\epsilon - s} \right\} [e]_+ [s]_+ \quad (28)$$

provided that  $a_1 a_4 > \frac{a_5 a_2}{1+b}$ , will render the origin of the error space attractive. Additionally, there exist a certain period of time  $t^*$ , after which the error is bounded by:

$$0 < e < \epsilon \quad (29)$$

**Proof:** The prove here is divided into four parts; in the first part, we need to show that when the initial condition  $e(0)$  is initiated in  $\mathcal{Q}^{(+)}$ ,  $e(t)$  will not leave a Positively Invariant Set (PIS)  $\Sigma$  defined by:

$$\Sigma = \{(e, z) : 0 < s < \epsilon, e(0) \in \Omega^{(+)}\} \quad (30)$$

Similarly in the second part, we need to show that when the initial condition  $e(0)$  is initiated in  $\mathcal{Q}^{(-)}$ ,  $e(t)$  will enter the PIS  $\Sigma$  in a finite time  $t^*$ , and stay there for all future time. While in third part, we will use the fact that  $\Sigma$  is a PIS to show that after  $t=t^*$  the error bound is as given in the inequality (29). Finally, part 4 is devoted to show that the sub system dynamic of  $x_2$  is Input to State Stable (ISS) where the term  $\phi(x_1)$  is considered as the input. The need for ISS property for the  $x_2$  subsystem is crucial in proving the stability of the closed loop system.

**Part 1:** Let  $e(0) \in \mathcal{Q}^{(+)}$ , then from Eq. (28),  $u = \frac{1}{G} \left\{ \lambda_n e + \lambda_s \frac{s}{\epsilon - |s|} \right\}$ . So, the dynamics of the sliding variable, from Eqns. (22) and (23), becomes;

$$\dot{z} = \lambda_n e \quad (31)$$

$$\dot{s} = -\lambda_s \frac{s}{\epsilon - |s|} + H(x, u) \quad (32)$$

The aim is to show that in this case the state  $(e, z)$  will not leave  $\Sigma$ . This can be done by firstly using Lyapunov function  $W(s)$ . So, let  $W(s) = \frac{1}{2} s^2$ , its time rate of change is;

$$\begin{aligned} \dot{W}(s) &= s \dot{s} = s \left\{ -\lambda_s \frac{s}{\epsilon - s} + H(x, u) \right\} \\ &\leq -\lambda_s \frac{s^2}{\epsilon - s} + s |H(x, u)| \\ &\leq -s \left\{ \lambda_s \frac{s}{\epsilon - s} - \hat{H} \right\} \end{aligned} \quad (33)$$

where,  $|H(x, u)| < \hat{H}$ .  $\dot{W}(s) < 0$  if  $\lambda_s \frac{s}{\epsilon - s} - \hat{H} > 0$ . By solving the inequality for  $s$ , we get that  $\dot{W}(s) < 0$  for  $s > \frac{\hat{H}\epsilon}{\lambda_s + \hat{H}}$ , which means also that  $s$  is ultimately bounded by  $s < \frac{\hat{H}\epsilon}{\lambda_s + \hat{H}} < \epsilon$ . To complete the proof that the state  $(e, z)$  will not leave  $\Sigma$ , we need to show that when the state initiated at the sliding manifold, it will never go to the negative side of  $s(s < 0)$ . This is seen in the next part of this proof. Accordingly, since  $s(0)=0$ , the system state is also bounded by the sliding manifold  $s=0$ . This proves that  $(e, z) \in \Sigma$  if  $e(0) \in \Omega^{(+)}$ .

**Part 2:** In this part of proof,  $e(0) \in \Omega^{(-)}$ , and from Eq. (23),  $u=0$ . Here we need to show that  $\Sigma$  is the attractive set. Namely,  $e=0$  is an attractive point.

$$\begin{cases} \dot{x}_1 = -a_1 x_1 + a_2 x_2 \\ \dot{x}_2 = -a_4 x_2 + \phi(x_1) \end{cases} \quad (34)$$

To show that  $e=0$  is an attractive point, simply we need first to show that the desired output  $y_r$  is larger than the equilibrium point  $x_e = (x_{1e}, x_{2e})$ . And secondly, the open loop system has a globally asymptotically stable (GAS) equilibrium point  $x_e$ . The origin is the equilibrium point of Eq. (34),  $(x_e=(0,0))$ , and  $y_r \geq x_e$  for any desired output  $y_r$ . To prove that origin is GAS, Eq. (34) is rewritten in the following form;

$$\dot{x} = Ax + B\hat{\phi}(x_1) \quad (35)$$

where,

$$A = \begin{bmatrix} -a_1 & a_2 \\ \frac{a_5}{1+b} & -a_4 \end{bmatrix}, \quad B = [0 \ 1],$$

$$\hat{\phi}(x_1) = \left( \frac{a_5}{1+be^{-x_1}} - \frac{a_5}{1+b} \right) x_1 = \psi(x_1)x_1, \text{ and } b = e^{a_6}$$

The matrix  $A$  is Hurwitz if and only if  $a_1 a_4 > \frac{a_5 a_2}{1+b}$ , which means that the origin is asymptotically stable. In the next step, we will use again the Lyapunov function based on the linear part of Eq. (35) to show that the origin is GAS. Since  $A$  is Hurwitz, then there exist a Lyapunov function  $\hat{V} = x^T P x$ , where  $P$  is the solution of the Lyapunov equation  $PA + A^T P = -I$ . The time derivative of  $\hat{V}$  is:

$$\dot{\hat{V}} = -\|x\|^2 + 2x^T P B \hat{\phi}(x_1) \leq -\|x\|^2 + 2\|x\| \|PB\| |\hat{\phi}(x_1)|$$

But  $|\hat{\phi}(x_1)| = \psi(x_1)x_1 < \gamma\|x\|, \gamma > 0$ , so we have:

$$\begin{aligned} \dot{\hat{V}} &< -\|x\|^2 + 2\gamma\|x\|^2 \|PB\| \\ &= -\|x\|^2 (1 - 2\gamma\|PB\|) \end{aligned} \quad (36)$$

Therefore,  $\dot{\hat{V}}$  is negative definite in the domain where  $\gamma < (1/2\|PB\|)$ . For the origin to be GAS, the inequality  $\gamma < (1/2\|PB\|)$  must be held globally, i.e.,  $\forall x \in R^2$ . Consequently, since  $e=0$  refers to the desired output  $y_r \geq x_e$ , then  $e=0$  is a globally attractive point for  $e(0) \in \Omega^{(-)}$ .

**Part 3:** From part 1,  $s=e+z < \epsilon, \forall t \geq 0$ , or  $e < \epsilon - z, \forall t \geq 0$ . So, in order to show that, eventually,  $e < \epsilon$ , we need to show that  $z < \epsilon, \forall t \geq 0$ .

From Eq. (31),  $z(t) = -e(0) + \lambda_n \int_0^t e(\sigma) d\sigma$ . As long as the error  $e$  is in  $\Omega^{(+)}$ ,  $z(t)$  increases until at a certain time  $t=t^*$ , at which  $z(t)$  becomes equal to zero, but then  $z(t) > 0 \forall t \geq t^*$ .

With proceeding of time, the ultimate value of  $z(t)$  will be  $\epsilon$ , and that if  $e$  goes to zero. Otherwise  $0 \leq z(t) < \epsilon, \forall t \geq t^*$ , and therefore,  $e < \epsilon, \forall t \geq t^*$ .

Also, with the aid of part 2, for  $e(0) \in \Omega^{(-)}$ ,  $t^*$  will be the time spent for the state to enter  $\Sigma$ . Again  $0 \leq z(t) < \epsilon, \forall t \geq t^*$ , and  $0 \leq e, \forall t \geq t^*$ , and by considering the inequality  $s = e + z < \epsilon, \forall t \geq t^*$ , inequality (29) is proved.

**Part 4:** This part is devoted to show that the closed loop system is stable in spite of the fact that the proposed controller was designed for the input-output model. In order to show that closed system is minimum phase and that  $e=0$  is an attractive point we need to show that  $x_2=0$  subsystem is ISS.

From Eq. (1), the dynamics of the  $x_2$  subsystem is given by;

$$\dot{x}_2 = -a_4 x_2 + \phi(x_1)$$

where,  $\phi(x_1)$  is treated as the input (or the external disturbance), while  $x_2$  as the state. The aim here is to show that during controlling the state variable  $x_1, x_2$  will be stable  $\forall t \geq 0$ , and ultimately will be equal to a steady state value of  $\phi(x_1)$ , i.e., equal to  $\phi(x_{1ss})$ .

The ISS property is tested via Lyapunov function  $\hat{W} = \frac{1}{2} x_2^2$ . The time derivative of  $\hat{W}$  is given by:

$$\begin{aligned} \dot{\hat{W}} &= x_2(-a_4 x_2 + \phi(x_1)) \\ &= -a_4 x_2^2 + x_2 \phi(x_1) \leq -a_4 x_2^2 + |x_2| |\phi(x_1)| \\ &\Rightarrow \dot{\hat{W}} \leq -a_4 x_2^2 + a_5 |x_2| |x_1| \end{aligned} \quad (37)$$

where,  $|\phi(x_1)| \leq a_5 |x_1|$ . Then the  $x_2$  subsystem is ISS because;

$$\begin{aligned} \dot{\hat{W}} &\leq -a_4 x_2^2 + a_5 |x_2| |x_1| \\ &\leq -a_4 (1 - \theta) x_2^2 - a_4 \theta x_2^2 + a_5 |x_2| |x_1| \\ &\leq -a_4 (1 - \theta) x_2^2, \quad \forall |x_2| > \frac{a_5}{a_4 \theta} |x_1| \end{aligned} \quad (38)$$

Therefore,  $x_2$  is a stable state and eventually bounded by  $\frac{a_5}{a_4} |x_{1ss}|$ .

As mentioned above, the chattering problem is the main obstacle that prevents the use of SMC for many applications. Although the controller which was proposed in this work is a continuous controller, accordingly, the chattering is eliminated. With the current positive control system ( $u=v^2 \geq 0$ ) the chattering appears again due to a discontinuity in the control law in Eq. (28). At  $e=0$ , the control law is discontinuous because;

$$u \in \left( 0, \frac{\hat{H}}{G} \right) \neq u(e=0) = 0 \quad (39)$$

In the following proposition, a simple modification is proposed to the control law given in Eq. (28) to remove the discontinuity and eliminate the chattering in the system response.

**Proposition 2:** For the HR response during treadmill exercise model (Eq. (1)), the control law:

$$u = \max \left( 0, \frac{1}{G} \left\{ \lambda_n e + \lambda_s \frac{s}{\epsilon - s} \right\} [s]_+ [e]_+ \right) \quad (40)$$

is a continuous controller, will render the origin of the error

space attractive provided that  $a_1 a_4 > \frac{a_5 a_2}{1+b}$ . Additionally, there exist a certain period of time  $t^*$ , after which the error is bounded by:

$$-\frac{\hat{H}}{\lambda_n} < e < \epsilon \quad (41)$$

**Proof:** We need first to show the control law in Eq. (40) as a continuous controller. In the proof of proposition 1, we show that  $\Sigma$  (see Eq. (30)) is a PIS. In this proposition, the PIS  $\hat{\Sigma}$  is given by:

$$\hat{\Sigma} = \{(e, z): 0 < s < \epsilon, e(0) \in \hat{\Omega}\} \quad (42)$$

where,  $\hat{\Omega}$  is given by:

$$\hat{\Omega} = \Omega^{(+)} \cup \{(e, z): e(0) \in \Omega^{(-)} u > 0\} \quad (43)$$

In other words,  $\hat{\Omega}$  consists of  $\Omega^{(+)}$  plus the set of points in  $\Omega^{(-)}$  where the control  $u$  is positive. Hence, the PIS  $\hat{\Sigma}$  is the set of points satisfying  $0 < s < \epsilon$  with a bound in  $\Omega^{(-)}$  by the loci of points that satisfied the condition  $u=0$ . This also means that outside  $\hat{\Omega}$ ,  $u=0$ . As a result, the control law in Eq. (40) is a continuous controller.

The remainder of the proof is as in the proof of Proposition 1.

#### 4. SIMULATION RESULTS

In this section, simulation results are illustrated to show the effectiveness of the proposed approach employing a typical time-varying HR reference profile. Scilab simulation platform is used for this purpose. ISMCbf in Eq. (40) is compared to QSMC designed in the study [14] and also to STSMC designed in the study [15]. The two controllers from the literature are employed here as designed in the original work but with the current output and error equation definitions. QSMC final design in the study [14] but for the output as given in Eq. (1) is as follows:

$$u_{QSMC} = \max\left(0, \frac{1}{a_3}(a_1 x_1 - a_2 x_2 + 0.25 \dot{y}_r + \rho \frac{s}{|s| + \epsilon_1})\right) \quad (44)$$

where,  $\rho = 2.121$ ,  $\dot{y}_r$  is the derivative of  $y_r$  [14],  $\epsilon_1 = 0.05$ . As for STSMC, the final control law is given as follows [15]:

$$u_{STSMC} = \max\left\{0, \frac{1}{a_3}(a_1 x_1 - a_2 x_2 + 0.25 \lambda e + 0.25 \dot{y}_r) + K|s|^\alpha \text{sign}(s)\right\} \quad (45)$$

where,  $K=10$ ,  $\alpha=0.5$  [15] and  $\lambda=1$ . These two control laws depend on the model parameters in Eq. (1). The nominal values of the parameters  $a_1$ ,  $a_2$ ,  $a_3$  are used here for the controllers QSMC and STSMC. The model parameters are considered to have uncertainty of  $\pm 10\%$  of the nominal values. Moreover, these two controllers require the derivative of the reference model ( $\dot{y}_r$ ) in their design. Any sudden change in  $y_r$  could possibly lead to an abrupt change in its derivative that appears in the control signal as an undesired impulsive effect. Moreover, QSMC and STSMC require the second state  $x_2(t)$  in their control laws. This adds the burden of estimating this

state to be able to use it. Conversely, ISMCbf uses only the available output state and does not require differentiating its desired reference in its control law. Therefore, ISMCbf design is simpler and the model parameters and their bounds are considered unknown in all simulation scenarios. Only one nominal value is taken and set fixed in all tests for all subjects that is  $a_{3n} = 0.7$  (less than the average values of  $a_3$  of five subjects in the research [15]). The design parameters of ISMCbf in Eq. (40) are set to  $\lambda_n = \lambda_s = 5(4 * a_{30})$ ,  $\epsilon = 0.5$ .

#### 4.1 Scenario I

In the first case study, the following parameter values of [11] are employed with maximum speed of  $v_{max} = 8$  km/h:  $a_1=2.2$ ,  $a_2=19.96$ ,  $a_3=0.38$ ,  $a_4=0.0831$ ,  $a_5=0.002526$ ,  $a_6=8.32$ . The desired HR reference profile is a 40 minutes typical training that has warm up/holding/cool down phases. The hold phase has two HR levels namely 110 and 120 bpm respectively. The warm-up period of the first HR profile is 3-minute period with a gradual increase from 74 bpm to 110 bpm (56 – 60% of maximal HR). Then the next 10 minutes HR is held at 110 bpm. The second 3-minutes gradual increase from 110 to 120 bpm. After 10 minutes of holding HR at 120 bpm, the cool-down phase starts firstly by a gradual decrease of HR to 110bpm then to the subject's recovery HR=74 bpm as shown in Figure 1. Two exercises from different initial condition are simulated. The initial condition in the first is set to  $x_1(0)=3$ ,  $x_2(0)=0$  i.e.  $y(0) = 86$  bpm with a consequently large positive initial HR regulation error ( $e(0)=-12$  bpm as set in the research [11]). In the second simulation, the initial condition is set to  $x_1(0)=-3$ ,  $x_2(0)=0$  with a large negative initial HR error ( $e(0)=-12$  bpm). The simulation results of these two cases are shown in Figures 1-6 respectively. The speed control action of the two cases is shown in Figures 2 and 5. As shown all three controllers give a satisfactory performance leading HR to follow the desired time-varying reference trajectory. However, ISMCbf confined the steady-state error in the barrier neighborhood from the first instant unlike QSMC and STSMC as shown in Figures 1, 3, 4 and 6. It is interesting to mention that HR did not completely follow the resting HR profile for the cool-down period for  $t > 30$  min as illustrated in Figure 1 and 4. This is due to the fact that the recovery HR of the subject can not be further reduced as the treadmill already stopped  $u=0$  km/h as shown in Figures 2 and 5. Similarly, at the beginning of the first exercise HR profile, with ISMCbf and STSMC, the treadmill started moving if a subject had a high resting HR as shown in Figure 2. Since the resting HR was higher than the desired HR, the resting HR of the subject can not be reduced by the controlled treadmill. Table 1 presents a quantitative comparison using two performance indices: Integral Square Error (ISE) and Integral Time absolute Error (ITAE) of the three controllers for the two exercises. These two indices were used [14] to compare classic SMC and QSMC performances.

**Table 1.** Performance analysis of ISMCbf, QSMC and STSMC of scenario I

Controller	ISE	ITAE
ISMCbf	Exercise a=198.03	Exercise a=1307.06
	Exercise b= 185.97	Exercise b=1306.8
QSMC	Exercise a=249.27	Exercise a=1321.50
	Exercise b=226.78	Exercise b=1319. 3
STSMC	Exercise a=200.34	Exercise a=1311.05
	Exercise b=190.63	Exercise b=1309.77

## 4.2 Scenario II

**Table 2.** Performance analysis of ISMCbf, QSMC and STSMC of scenario II-subject1

Controller	ISE	ITAE
ISMCbf	18.22	222.45
QSMC	11292.53	10793.19
STSMC	19.83	232.88

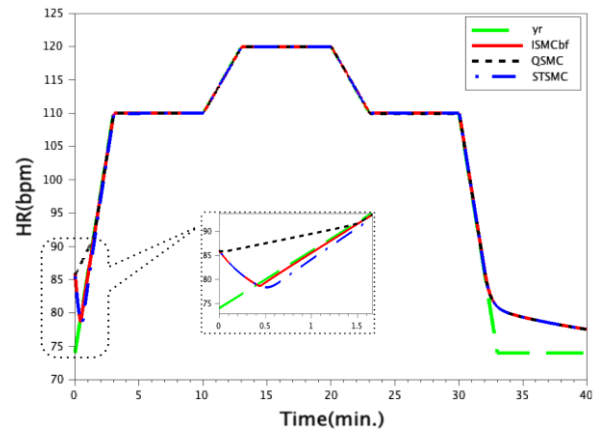
**Table 3.** Performance analysis of ISMCbf, QSMC ( $2\rho$ ) and STSMC of scenario II for four subjects

Controller	ISE	ITAE
ISMCbf	Sub.2=09.41	Sub.2=134.44
	Sub.3=11.27	Sub.3=152.25
	Sub.4=11.13	Sub.4=152.42
	Sub.5=11.9	Sub.5=162.7
	Sub.2= 34.28	Sub.2=247.12
QSMC	Sub.3=34.83	Sub.3=212.17
	Sub.4=35.62	Sub.4=241.34
	Sub.5=38.24	Sub.5=300.38
	Sub.2 = 11.03	Sub.2=143.9
	Sub.3=12.94	Sub.3=160.62
STSMC	Sub.4=12.79	Sub.4=162.36
	Sub.5=13.56	Sub.5=173.71

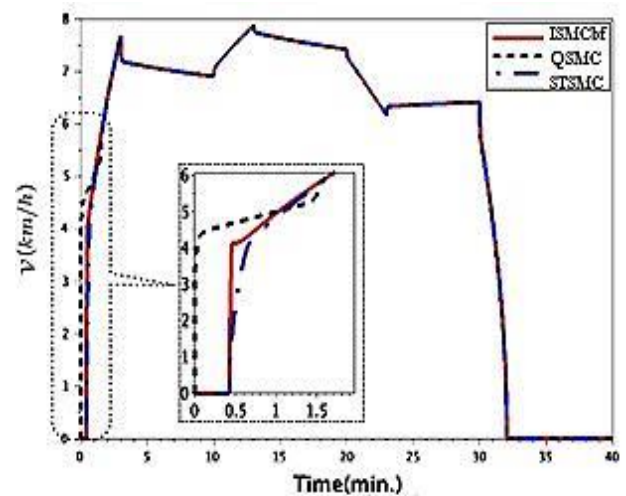
In this scenario, the desired exercise profile for higher HR levels using larger speed range ( $v \leq 14$  km/h) whose parameters are estimated [15] for different subjects. The exercise profile includes warm up, holding and cool down phases. The warm up starts from resting HR and increases gradually to 100 bpm for three minutes followed by a gradual increase to 120 bpm held for three minutes then increases to 135 bpm and held there for seven minutes. The recovery cool down phase starts in a reverse manner by a gradual HR decrease to finally reach  $HR_0$  as illustrated in Figure 7. The full exercise duration is 40 minutes. The initial condition is  $x_1(0)=-3$ ,  $x_2(0)=0$ . The exercise is tested on subject number 1 [15] whose parameters are  $a_1=2.512$ ,  $a_2=25.92$ ,  $a_3=.81$ ,  $a_4=.902$ ,  $a_5=0.038$ ,  $a_6=5.37$ ,  $HR_0=64$ . The three controllers ISMCbf, QSMC and STSMC are compared using the same previous set of design parameters presented earlier. The nominal model parameters for QSMC and STSMC are different from the actual parameters by  $\pm 10\%$ . As shown in Figure 7, HR followed the new extensive exercise under ISMCbf and STSMC while QSMC performance was degraded in this scenario. The speed of the three controllers behaviors are shown in Figure 8. It is good to mention that QSMC was designed and tested [14] on a lower treadmill speed model of 8km/h and thus for lower HR levels. Figure 9 shows the sliding surfaces of the three controllers where QSMC surface attractiveness condition is violated in this scenario. This is due to the fact that the control gain  $\rho$  in Eq. (39) for QSMC has to be increased to fulfill the new higher desired HR levels.

Table 2 presents the performance ISE and ITAE indices for the three controllers in this scenario. The comparison is re-established for four other subjects (Sub.2-5) whose parameters are provided in the research [15]. For a fair comparison, in these cases QSMC gain is doubled to fulfill the attractiveness condition  $\rho=4.24$ . Table 3 illustrates the four subjects' quantitative results of the three control laws. ISMCbf dominated other controllers' performances recalling that its design procedure is simpler and does not require any prior information about the system model parameters nor their uncertainties bounds. Moreover, unlike QSMC it does not

have a discontinuous term and thus it is a chattering-free controller.



**Figure 1.** HR profile of scenario I-a: dashed green line for the desired profile, solid red line for ISMCbf control, dotted black line for QSMC, dash-dot blue line for STSMC



**Figure 2.** Speed of the treadmill (control input) of scenario I-a: solid red line for ISMCbf control, dotted black line for QSMC, dash-dot blue line for STSMC

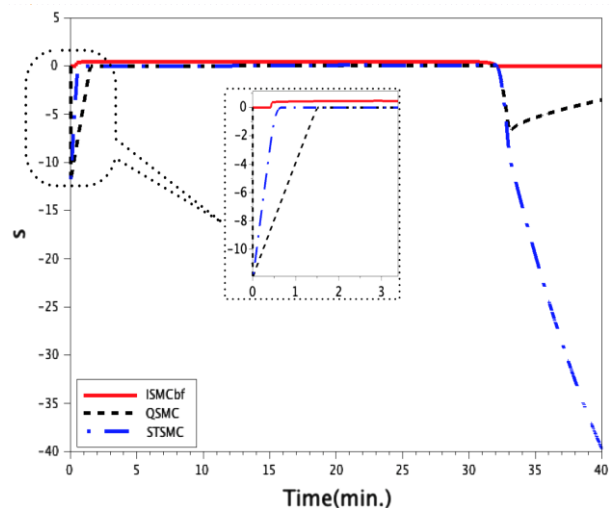


**Figure 3.** Sliding surface of each control input of scenario I-a: solid red line for ISMCbf control, dotted black line for QSMC, dash-dot blue line for STSMC

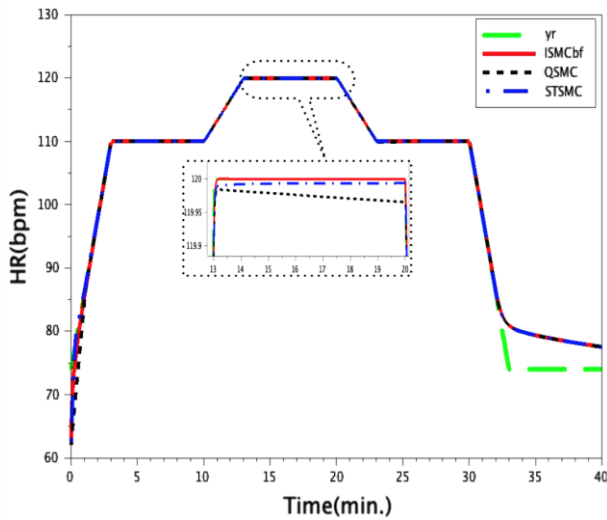


**Figure 4.** HR profile of scenario I-b: dashed green line for the desired profile, solid red line for ISMCbf control, dotted black line for QSMC, dash-dot blue line for STSMC

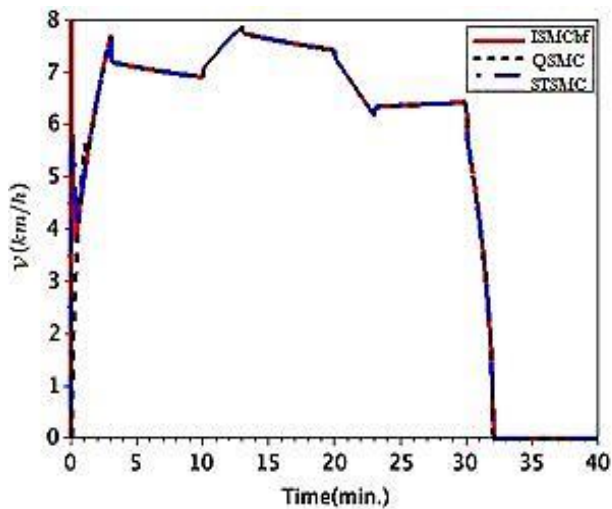


**Figure 5.** Speed of the treadmill (control input) of scenario I-b: solid red line for ISMCbf control, dotted black line for QSMC, dash-dot blue line for STSMC

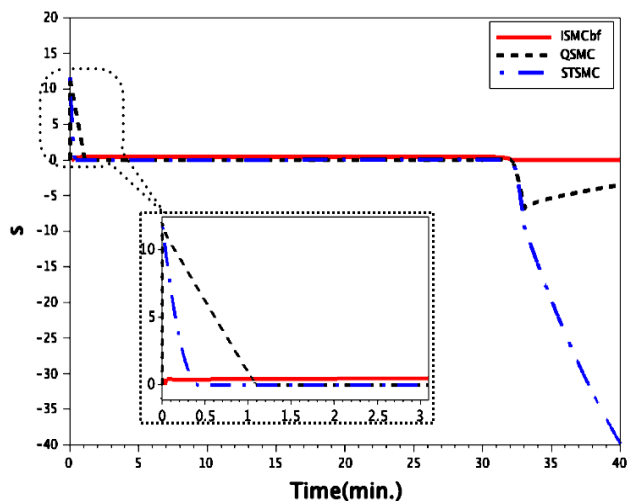


**Figure 6.** Sliding surface of each control input of scenario I-b: solid red line for ISMCbf control, dotted black line for QSMC, dash-dot blue line for STSMC

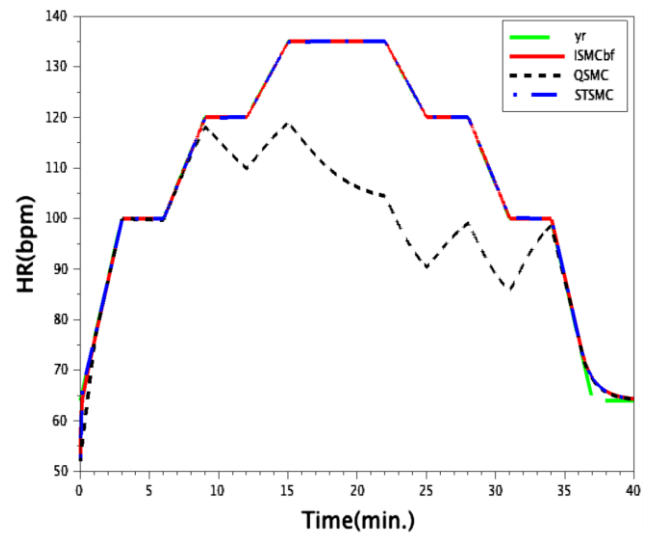


**Figure 7.** HR profile of scenario II: dashed green line for the desired profile, solid red line for ISMCbf control, dotted black line for QSMC, dash-dot blue line for STSMC

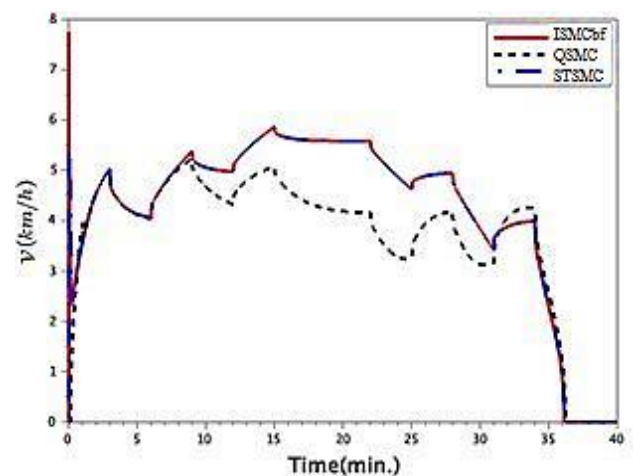


**Figure 8.** Speed of the treadmill (control input) of scenario II: solid red line for ISMCbf control, dotted black line for QSMC, dash-dot blue line for STSMC

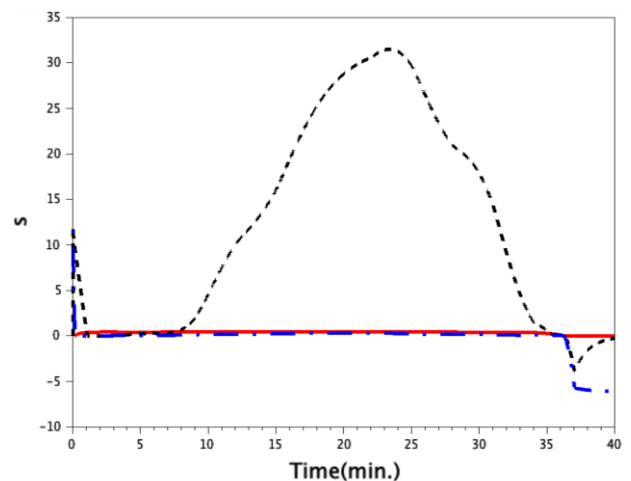


**Figure 9.** Sliding surface of each control input of scenario II: solid red line for ISMCbf control, dotted black line for QSMC, dash-dot blue line for STSMC

## 5. CONCLUSION

In this work, ISMCbf is designed for the first time to control HR response during treadmill exercise. The control problem is to steer HR to follow a pre-specified exercise profile prescribed by physicians as part of a cardiac rehabilitation program. The controller suitably decides the treadmill speed according to the HR regulation error and without any prior knowledge of the model parameters, uncertainties bounds nor nonlinearities. ISMCbf is chosen due to its high robustness and simple design as compared to classical SMC where the bounds of uncertainties should be given in the design. Moreover, ISMCbf is continuous and chattering-free controller. The output tracking accuracy and steady-state error is decided by selecting a small positive parameter that defines the barrier invariant set. In this set the state trajectory is confined to achieve the required performance. ISMCbf is compared to two other robust controllers designed in the literature: QSMC and STSMC. The comparison is conducted in two different scenarios applied on a nonlinear HR model during treadmill exercises. Two different desired exercise profiles are used, one for maximum treadmill speed of 8km/h and in the second is for more intensive HR exercise profile. The main advantages of ISMCbf as compared to QSMC and STSMC are summarized as follows:

1. It does not require any prior knowledge of model parameters nor their uncertainty bounds.
2. QSMC and STSMC employed the derivative of the reference model ( $y_r$ ) in the control law. Any sudden change in  $y_r$  could possibly lead to an undesired impulsive change in its derivative that appears in the control signal.
3. QSMC and STSMC used the second state  $x_2(t)$  in their control laws. This adds the burden of estimating this state to be able to use it in the control law.
4. ISMCbf is chattering-free because it is inherently continuous and does not need any approximation for the discontinuous term in SMC. ISMCbf and STSMC is chattering-free but the former is much simpler in its design.

Future suggestions could be to test the design experimentally in practice. ISMCbf for systems under input/output constraints in general deserves further attention and development.

## REFERENCES

- [1] World Health Organization, Cardiovascular Diseases (CVDs), 11 June, 2021. [https://www.who.int/en/news-room/fact-sheets/detail/cardiovascular-diseases-\(cvds\)](https://www.who.int/en/news-room/fact-sheets/detail/cardiovascular-diseases-(cvds)).
- [2] Winnige, P., Vysoky, R., Dosbaba, F., Batalik, L. (2021). Cardiac rehabilitation and its essential role in the secondary prevention of cardiovascular diseases. *World Journal of Clinical Cases*, 9(8): 1761-1784. <https://doi.org/10.12998%2Fwjcc.v9.i8.1761>
- [3] Cheng, T.M., Savkin, A.V., Celler, B.G., Su, S.W., Wang, L. (2008). Nonlinear modeling and control of human heart rate response during exercise with various work load intensities. *IEEE Transactions on Biomedical Engineering*, 55(11): 2499-2508. <https://doi.org/10.1109/TBME.2008.2001131>
- [4] Zakyntinaki, M.S. (2015). Modelling heart rate kinetics. *PloS One*, 10(4): e0118263. <https://doi.org/10.1371/journal.pone.0118263>
- [5] Ni, J., Muhlstein, L., McAuley, J. (2019). Modeling heart rate and activity data for personalized fitness recommendation. In *The World Wide Web Conference*, pp. 1343-1353. <https://doi.org/10.1145/3308558.3313643>
- [6] Ludwig, M., Hoffmann, K., Endler, S., Asteroth, A., Wiemeyer, J. (2018). Measurement, prediction, and control of individual heart rate responses to exercise—Basics and options for wearable devices. *Frontiers in Physiology*, 9: 778. <https://doi.org/10.3389/fphys.2018.00778>
- [7] Wang, H., Hunt, K.J. (2021). Identification of heart rate dynamics during treadmill exercise: comparison of first- and second-order models. *BioMedical Engineering Online*, 20: 1-10. <https://doi.org/10.1186/s12938-021-00875-7>
- [8] Spörri, A.H., Wang, H., Hunt, K.J. (2022). Heart rate dynamics identification and control in cycle ergometer exercise: Comparison of first- and second-order performance. *Frontiers in Control Engineering*, 3: 1-9. <http://dx.doi.org/10.3389/fcteg.2022.894180>
- [9] Paradiso, M., Pietrosanti, S., Scalzi, S., Tomei, P., Verrelli, C.M. (2012). Experimental heart rate regulation in cycle-ergometer exercises. *IEEE Transactions on Biomedical Engineering*, 60(1): 135-139. <https://doi.org/10.1109/TBME.2012.2225061>
- [10] Liu, X., Su, X., Tamminen, S., Korhonen, T., Röning, J. (2019). Predicting the heart rate response to outdoor running exercise. In *2019 IEEE 32nd International Symposium on Computer-Based Medical Systems (CBMS)*, pp. 217-220. <https://doi.org/10.1109/CBMS.2019.00052>
- [11] Scalzi, S., Tomei, P., Verrelli, C.M. (2011). Nonlinear control techniques for the heart rate regulation in treadmill exercises. *IEEE Transactions on Biomedical Engineering*, 59(3): 599-603. <https://doi.org/10.1109/TBME.2011.2179300>
- [12] Baig, D.E.Z., Ahmad, R., Savkin, A., Celler, B. (2019). Robust adaptive  $H_\infty$  control design for heart rate regulation during rhythmic exercises of unknown type. *International Journal of Adaptive Control and Signal Processing*, 33(5): 843-854. <https://doi.org/10.1002/acs.2992>
- [13] Argha, A., Su, S.W., Nguyen, H.T., Celler, B.G. (2015). Designing adaptive integral sliding mode control for heart rate regulation during cycle-ergometer exercise using bio-feedback. 2015 37th Annual International Conference of the IEEE Engineering in Medicine and Biology Society (EMBC), pp. 6688-6691. <https://doi.org/10.1109/EMBC.2015.7319927>
- [14] Sarkar, S., Sengupta, A. (2018). Quasi sliding mode control: An application to heart rate regulation. 2018 International Conference on Control, Power, Communication and Computing Technologies (ICCPCTT), Kannur, India, pp. 299-304. <https://doi.org/10.1109/ICCPCTT.2018.8574263>
- [15] Esmaili, A., Ibeas, A., Herrera, J., Esmaili, N. (2019). Identification and robust control of heart rate during treadmill exercise at large speed ranges. *Journal of Control Engineering and Applied Informatics*, 21(1): 51-60.
- [16] Obeid, H., Fridman, L.M., Laghrouche, S., Harmouche, M. (2018). Barrier function-based adaptive sliding mode control. *Automatica*, 93: 540-544.

<https://doi.org/10.1016/j.automatica.2018.03.078>

[17] Liu, Z., Pan, H. (2020). Barrier function-based adaptive sliding mode control for application to vehicle suspensions. *IEEE Transactions on Transportation Electrification*, 7(3): 2023-2033. <https://doi.org/10.1109/TTE.2020.3043581>

[18] Abd, A.F., Al-Samarraie, S.A. (2021). Integral sliding mode control based on barrier function for servo actuator with friction. *Engineering and Technology Journal*, 39(2): 248-259. <https://doi.org/10.30684/etj.v39i2A.1826>

[19] Husain, S.S., MohammadRidha, T. (2022). Integral sliding mode controlled ATMD for buildings under seismic effect. *International Journal of Safety and Security Engineering*, 12(4): 413-420. <http://dx.doi.org/10.18280/ijss.120401>

[20] Utkin, V., Guldner, J., Shi, J. (2009). *Sliding Mode Control in Electro-Mechanical Systems* (2nd ed.). CRC Press. <https://doi.org/10.1201/9781420065619>

[21] Utkin, V., Shi, J. (1996). Integral sliding mode in systems operating under uncertainty conditions. In *Proceedings of 35th IEEE Conference on Decision and Control*, vol. 4, pp. 4591-4596. <https://doi.org/10.1109/CDC.1996.577594>

[22] Castaños, F., Fridman, L. (2006). Analysis and design of integral sliding manifolds for systems with unmatched perturbations. *IEEE Transactions on Automatic Control*, 51(5): 853-858. <https://doi.org/10.1109/TAC.2006.875008>

[23] Utkin, V.I. (2013). *Sliding Modes in Control and Optimization*. Springer Science & Business Media. <https://doi.org/10.1007/978-3-642-84379-2>

[24] Utkin, V. (1977). Variable structure systems with sliding modes. *IEEE Transactions on Automatic Control*, 22(2): 212-222. <https://doi.org/10.1109/TAC.1977.1101446>

## NOMENCLATURE

HR	Hear Rate
PIS	Positively Invariant Set

## Greek symbols

$\epsilon, \epsilon_1$	Small design parameter
$\lambda, \lambda_s, \lambda_n$	Positive design parameters
$\Omega^{(+)}, \Omega^{(-)}$	Sets where $e > 0$ , $e < 0$ respectively
$\Sigma$	A Positively Invariant Set